

1 **Behavioural and life-history responses of mosquitofish to**  
2 **biologically-inspired and interactive robotic predators**

3

4 Giovanni Polverino, Mert Karakaya, Chiara Spinello, Vrishin R. Soman, Maurizio Porfiri

5

6

7

8

**SUPPLEMENTARY MATERIAL**

9

## 10 **MATERIALS AND METHODS**

### 11 **Robotic platform and bioinspired predator replicas**

12 A robotic platform with three degrees of freedom was utilized to actuate the predator  
13 replica in the experimental arena. A total of three stepper motors were installed on the  
14 platform and two of them were used to translate the replica on the X-Y Cartesian plane,  
15 while the third motor was used to adjust the orientation of the fish. This mechanism  
16 allowed for mimicking in the swimming pattern of live basses in shallow waters. Starting  
17 with a commercially available Cartesian plotter (XY Plotter Robot Kit, Makeblock Co., Ltd,  
18 Shenzhen, China), we included a third stepper motor (NEMA 14, Pololu Corp., Las Vegas, NV,  
19 USA) on the end effector of the Cartesian plotter using a 3-D printed bracket. To control the  
20 motors and allow communication with the computer, we used a dedicated microcontroller  
21 for each motor (Kuman CNC Kit, Kuman Trade Co., Shenzhen, China). To interface each  
22 microcontroller with the computer, we utilized GRBL 0.9 tool (Grbl™ v0.9, Copyright (c)  
23 2012-2014 Sungeun K. Jeon) and we used Matlab R2018 (The MathWorks, Inc., Natick, MA,  
24 USA) to establish serial communication regarding position, speed, and turn rate data with  
25 the platform.

26

### 27 **Experimental conditions and live tracking**

28 To capture the position of the live fish and implement the closed-loop conditions (CL1 and  
29 CL2), a real-time tracking and control system was developed based on the computer vision  
30 toolbox in Matlab R2018 (The MathWorks, Inc., Natick, MA, USA). The tracking algorithm  
31 was a motion-based multiple object tracking. Specifically, focusing on a predetermined  
32 region of interest, an initial frame was obtained, cropped, and converted into a black and  
33 white image. Then, this initial frame was subtracted from the instantaneous frame to form a  
34 image mask. After filtering noise, the mask was utilized to identify the focal mosquitofish,  
35 whereby blob analyses were performed to track the centroids of the fish over time (trial).

36 If the system failed to identify the position of the focal fish, the position would be  
37 predicted by a Kalman filter based on the history of the trajectory, under constant velocity  
38 assumption. To help monitor the experimental procedure, two indicators were  
39 implemented to identify whether the robot was attacking or swimming and whether its  
40 distance from the fish was larger or smaller than 5 cm.

41

42 **Data processing**

43 Trajectories of mosquitofish and replicas were extracted from the videos to gather  
44 information on both behaviours and positions of fish and replicas. First, the obtained  
45 trajectories were smoothed using Gaussian smoothing with a moving window of 30 frames  
46 (1.5 s) to reduce measurement noise. Then, the smoothed data was processed to estimate  
47 distance moved (in cm), freezing (in s), speed variance during swimming (in  $\text{cm}^2/\text{s}^2$ ), and  
48 mean distance from the replica (in cm) at each minute of a trial.

49 To calculate the total distance moved, the distance moved in each time frame (0.05 to  
50 904 s) was calculated by taking the norm of the vector between positions in consecutive  
51 frames. The same distance was divided by the time step (0.05 s) to obtain the instantaneous  
52 speed, which we used to isolate freezing instances. Freezing instances were excluded from  
53 the overall observation to compute the mean speed and speed variance. The distance of the  
54 fish from the replica was calculated by taking norm of the vector between the fish position  
55 and replica position. Then, the mean values of the distances were computed for each  
56 minute of the trial as well as for the overall trial.

57

58 **RESULTS**

59 **Table S1 Phenotypic-correlation estimates between pairs of traits (body length, mass, and**  
60 **Fulton's  $K$ ).**

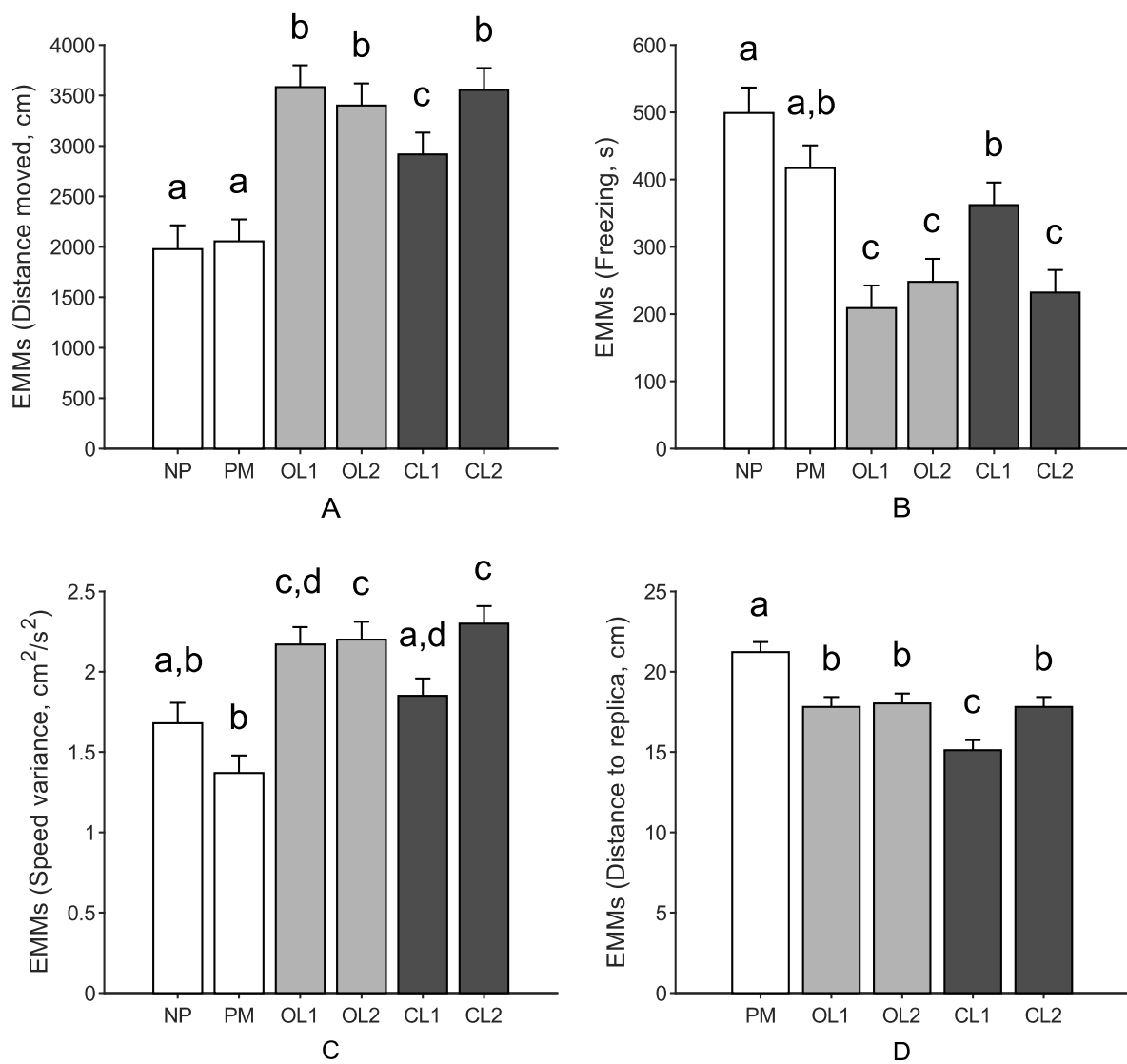
	Body length	Body mass	$K$
Body length	-	<b>0.624</b>	<b>-0.344</b>
Body mass	0.499; 0.745	-	-0.013
$K$	-0.492; -0.176	-0.184; 0.151	-

61 The best estimate of correlation coefficients (values above the diagonal) and their 95%  
62 credible intervals (values below the diagonal) are represented for each pair of traits. We  
63 used bivariate linear mixed-effects models using Markov Chain Monte Carlo techniques,  
64 including the individual as a random effect (that is, random intercepts) to account for  
65 repeated measures. Significant results correspond to correlation coefficients whose credible  
66 intervals do not overlap with zero (highlighted in bold).

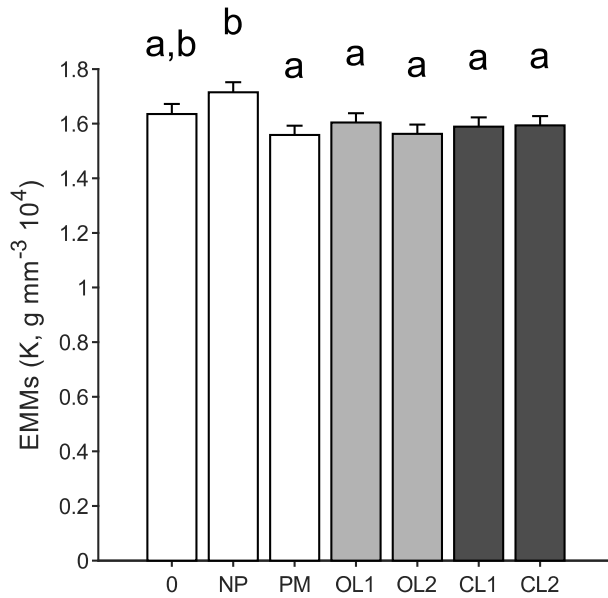
67 **Table S2 Results from LMMs with Fulton's *K* (body condition) as the dependent variable.**

<i>K</i>				
Fixed factors	Mean Sq	<i>df</i>	<i>F</i>	<i>P</i>
Sex	0.009	1, 71	0.507	0.479
Week	0.927	1, 436	50.036	<0.001***
Condition	0.185	6, 436	9.990	<0.001***
Random effects	Estimate (SE)	$\Delta$ AIC	$\chi^2_1$	<i>P</i>
$V_{\text{among}}$	0.018 ()	186.667	188.667	<0.001***
$V_{\text{within}}$	0.018 ()			
Repeatability	0.488			

68 Sex, week, and condition are included in the models as fixed factors, while random  
 69 intercepts are included for each individual, which allowed variance decomposition. Within-  
 70 individual variance ( $V_{\text{within}}$ ), among-individual variance ( $V_{\text{among}}$ ), and repeatability are shown.  
 71 Test statistics ( $\chi^2_1$ ) and significant levels of the random effects (i.e., intercepts) were  
 72 estimated using a LRT (*P*) and Akaike Information Criteria (AICs) between the full and the  
 73 null model. Note that  $\Delta$ AIC corresponds to the difference in AIC between the null models  
 74 minus the AIC from the full model. The significance was set at  $\alpha < 0.05$ , and significant results  
 75 are indicated with \*\*\* (<0.001).



76 **Figure S1** Estimated marginal mean (EMMs) differences represent adjusted mean  
 77 differences (+ SE) in distance moved, freezing, speed variance, and distance from the replica  
 78 across conditions once the contribution of fixed effects included in the model (that is,  
 79 Fulton's *K*, body mass, sex, week) is accounted for. White histograms correspond to control  
 80 conditions (NP and PM), light grey histograms to open-loop conditions (OL1 and OL2), and  
 81 dark grey histograms to closed-loop conditions (CL1 and CL2). Means not sharing a common  
 82 superscript are significantly different. The significance was set at  $\alpha < 0.05$ .



83

84 **Figure S2** Estimated marginal mean (EMMs) differences represent adjusted mean  
 85 differences (+ SE) in body condition (Fulton's *K*) across conditions once the contribution of  
 86 fixed effects included in the model (that is, sex, week) is accounted for. Notably, the first  
 87 histogram (0) refers to the baseline body condition measured before the beginning of the  
 88 experiment. White histograms correspond to control conditions (0, NP, and PM), light grey  
 89 histograms to open-loop conditions (OL1 and OL2), and dark grey histograms to closed-loop  
 90 conditions (CL1 and CL2). Means not sharing a common superscript are significantly  
 91 different. The significance was set at  $\alpha < 0.05$ .